EEG Signal Modeling Using Adaptive Markov Process Amplitude

Hasan Al-Nashash, *Senior Member, IEEE*, Yousef Al-Assaf, Joseph Paul, and Nitish Thakor*, *Fellow, IEEE*

***Abstract*—In this paper, an adaptive Markov process amplitude algorithm is used to model and simulate electroencephalogram (EEG) signals. EEG signal modeling is used as a tool to identify pathophysiological EEG changes potentially useful in clinical diagnosis. The least mean square algorithm is adopted to continuously estimate the parameters of a first-order Markov process model. EEG signals recorded from rodent brains during injury and recovery following global cerebral ischemia are utilized as input signals to the model. The EEG was recorded in a controlled experimental brain injury model of hypoxic-ischemic cardiac arrest. The signals from the injured brain during various phases of injury and recovery were modeled. Results show that the adaptive model is accurate in simulating EEG signal variations following brain injury. The dynamics of the model coefficients successfully capture the presence of spiking and bursting in EEG.**

***Index Terms*—Cardiac arrest, EEG, Markov process, signal modeling.**

I. Introduction

IN THE United States, cardiac arrest (CA) affects around 500 000 individuals per year [1]. Recent technological developments of implantable and portable defibrillators have resulted in a successful resuscitation of many patients in or outside the hospital. However, a large majority of resuscitated patients are left with significant neurological impairment. Neuronal damage from CA occurs within minutes and rapidly devastates brain function with permanent consequences shortly after its onset. We are now in a situation where the heart is functioning but the brain is damaged. Furthermore, the lack of sensitive detection and monitoring methods has impeded clinical investigations into improving diagnosis and recovery of brain function. Dramatic improvements in quantitative measures of brain injury severity have been demonstrated. Still, the overall compelling goal is to bring to the bedside state-of-the art instrumentation for rapid and accurate detection of brain injury severity and progression in CA victims [2].

Despite the many applications of EEG in clinical neurophysiology [3]–[8], its visual interpretation is very subjective and does not lend itself to statistical analysis. As a result, a number of research groups have proposed methods to quantify the information content of the EEG. Among these are the Fourier transform, the wavelet transform, chaos, entropy, and subband wavelet entropy [9]–[13]. In addition, EEG signal modeling is important to achieve a better understanding of the physical mechanisms generating these signals and to identify the causes of EEG signals changes [14]. Furthermore, pattern recognition and classification of EEG abnormalities can be achieved through the analysis of the estimated model parameters. Modeling can also be used for predicting the future neurological outcome and for data compression. Simulation based on EEG signal model can be used to better demonstrate the effectiveness of a certain quantitative analysis method or EEG feature extraction system.

Bai *et al.* [14] have developed a first-order Markov process amplitude (MPA) expressed by the sinusoidal waves to model the EEG signal. The parameters of the model were determined using frequency analysis to maximize the similarities between original and simulated EEG signals' power spectral densities (PSDs). Results showed that with few parameters, the MPA EEG model can represent the features of stationary EEG segments in time and frequency domains.

The MPA EEG model is applicable to stationary EEG signals. However, in our experimental setting of recovering EEG, the EEG signal is highly nonstationary. An accurate estimation of fixed MPA model parameters may therefore not be possible. Several studies have shown that adaptive filtering is suitable for analyzing time-varying signals [16], [17]. In this paper, we present an adaptive EEG signal model based on MPA where some model parameters are determined adaptively using the least mean square (LMS) algorithm [17]. The model should free us from the stationarity constraints and the need to repeatedly and manually calculate the MPA model parameters. Further, since the EEG signal is nonstationary, the adaptive estimation of model parameters should reflect and detect the changes in EEG measured during the various phases of recovery following a short instance of cerebral injury created using hypoxic/asphyxic CA in a rodent model.

The paper is organized as follows. In Section II, the experimental setup and protocol followed by the data collection and preprocessing are described. Next, the adaptive algorithm for the MPA EEG model is derived. In Section III, we describe the implementation of the algorithm with some simulation results. Finally, conclusions and suggestions for future work are also included in Section IV.

Manuscript received October 4, 2002; revised May 11, 2003. This work was supported in part by the National Institutes of Health (NIH) under Grant NS24282 and Grant NS42690 and in part by the AUS under Grant 1/2001. *Asterisk indicates corresponding author.*

H. Al-Nashash and Y. Al-Assaf are with the School of Engineering, American University of Sharjah, Sharjah, U.A.E.

J. Paul is with the Department of Biomedical Engineering, The Johns Hopkins School of Medicine, Baltimore, MD 21205 USA.

*N. Thakor is with the Department of Biomedical Engineering, The Johns Hopkins School of Medicine, Baltimore, MD 21205 USA (e-mail: nthakor@bme.jhu.edu).

Digital Object Identifier 10.1109/TBME.2004.826602

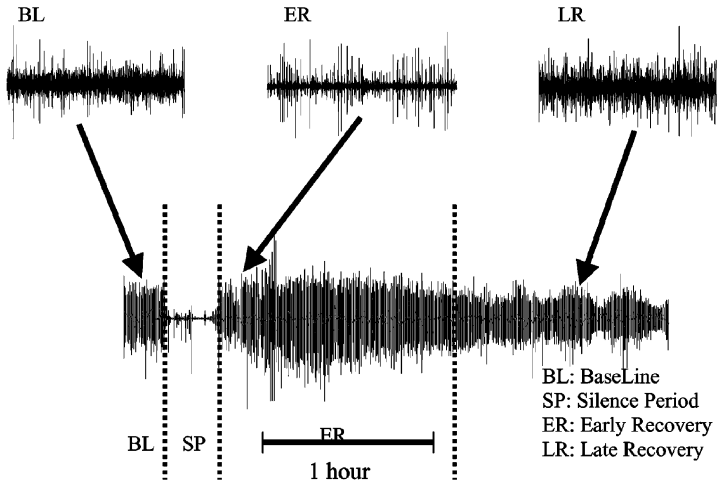

Fig. 1. EEG signal record for a period of 200 min. The EEG recording is divided into four parts: base line (BL), silent period (SP), early recovery (ER), and late recovery (LR).

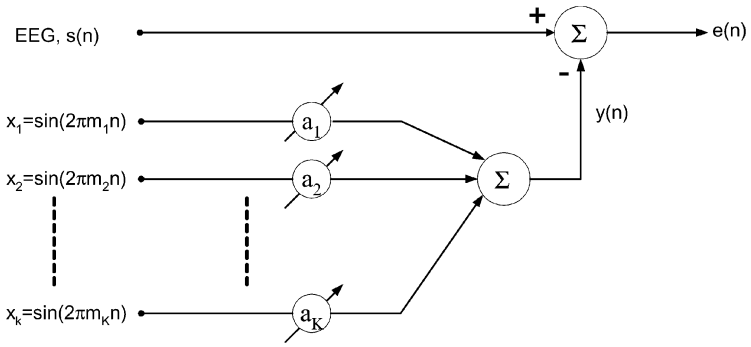

Fig. 2. Block diagram of the adaptive MPA combiner of the AMPA algorithm.

II. Methodology

A. Protocol

Long-term EEG was recorded from awake behaving rats after being subjected to controlled periods of asphyxia and CA using the asphyxic CA and resuscitation protocol as modified from Katz and colleagues [18]. The electrodes were screwed in place after the rats were anesthetized with Halothane. The asphyxia protocol was initiated with a 5-min anesthetic washout period. Asphyxia was induced by stopping the ventilator and clamping the ventilator tubes for controlled time duration. Resuscitation was initiated by resuming mechanical ventilation of 100% O_2 at 90 breaths/min and performing Cardio Pulmonary Resuscitation (CPR). When a spontaneous mean arterial blood pressure more than 50 mmHg was achieved indicating return of spontaneous circulation, CPR was stopped. After one hour of recovery, rats were extubated and allowed to breathe spontaneously.

B. Data Collection and Preprocessing

The EEGs were recorded from two differential channels from the left and right fronto-parietal regions of the rat's brain. The signals were lowpass filtered with 100-Hz cutoff frequency prior sampling with 250 samples per second and digitization using a 12-bit A/D converter. Fig. 1 shows the EEG signal recorded for a period of 200 min. The EEG recording is divided into four parts: before asphyxic arrest [BaseLine (BL)], asphyxic CA [Silence Period (SP)], Early Recovery (ER), and Late Recovery (LR) periods. The figures in the inset represent typical Baseline (BL) EEG segments prior to injury, during early and late periods of recovery (ER, LR). The ER period is generally characterized by a spiking activity while the LR period is characterized by bursting activity and general restoration of a continuous rhythm.

C. Adaptive MPA (AMPA) EEG Model

Fig. 2 shows a block diagram of the AMPA EEG model of K sinusoidal waves. The estimated EEG output $y(n)$ is composed of K different oscillations (x_j, $j = 1, 2, \ldots, K$)

$$y(n) = \sum_{j=1}^{K} a_j(n) x_j(n) = \sum_{j=1}^{K} a_j(n) \sin(2\pi m_j n + \phi_j) \quad (1)$$

where $a_j(n)$ is the model amplitude of the first-order Markov process, m_j is the dominant jth frequency, ϕ_j is the initial phase which was assumed to be equal to zero, and n is the time index. The next estimate of the model amplitude $a_j(n+1)$ is defined as

$$a_j(n+1) = \gamma_j(n) a_j(n) + \mu_j(n) \xi_j(n), \quad j = 1, 2, \ldots K \quad (2)$$

where $\xi_j(n)$ is the independent increment of Gaussian distribution with zero mean and unity variance. μ_j is the coefficient of the random process and γ_j is the coefficient of the first-order

Markov process. It can be shown that γ_j should satisfy the condition $0 < \gamma_j < 1$ for model stability.

If $s(n)$ is the EEG signal to be modeled, then the instantaneous error of the adaptive system is defined as

$$e(n) = s(n) - y(n). \tag{3}$$

The least-mean-square algorithm uses the mean square error (MSE) cost function defined as

$$\begin{aligned} J &= \frac{1}{2}E\left(e(n)^2\right) = \frac{1}{2}E\left((s(n)-y(n))^2\right) \\ &= \frac{1}{2}Rs - \sum_{j=1}^{K} a_j(n)Rsx_j \\ &\quad + \frac{1}{2}\sum_{i=1}^{K}\sum_{j=1}^{K} a_i(n)a_j(n)Rxx_{i,j} \\ &= \frac{1}{2}Rs - \sum_{j}^{K}\Big(\gamma_j(n-1)a_j(n-1) \\ &\qquad + \mu_j(n-1)\xi_j(n-1)\Big)Rsx_j \\ &\quad + \frac{1}{2}\sum_{i=1}^{K}\sum_{j=1}^{K}\Big(\gamma_i(n-1)a_i(n-1)+\mu_i(n-1)\xi_i(n-1)\Big) \\ &\quad \times \Big(\gamma_j(n-1)a_j(n-1)+\mu_j(n-1)\xi_j(n-1)\Big)Rxx_{i,j} \end{aligned} \tag{4}$$

where $Rs = E\left(s(n)^2\right)$, $Rsx_j = E(x_j(n)s(n))$ and $Rxx_{i,j} = E(x_i(n)x_j(n))$.

To adaptively adjust γ and μ, the LMS algorithm introduced by Widrow [13] is used as shown in Fig. 3. The error squared, $e(n)^2$ itself was used as an estimate of $J(n)$. Therefore, we can specify a steepest descent type adaptive algorithms at each iteration for γ as

$$\gamma_j(n+1) = \gamma_j(n) - \eta_\gamma \hat{\nabla}_{\gamma_j} J(n) \tag{5}$$

where η_γ is a small positive constant called the adaptive learning rate which controls the speed of the adjustment and $\hat{\nabla}_{\gamma_j} J(n)$ is the average gradient approximation of $J(n)$ and is defined as

$$\hat{\nabla}_{\gamma_j} J(n) = \begin{bmatrix} \frac{\partial e^2(n)}{\partial \gamma_1(n-1)} \\ \vdots \\ \frac{\partial e^2(n)}{\partial \gamma_K(n-1)} \end{bmatrix}$$

$$\begin{aligned} \hat{\nabla}_{\gamma_j} J(n) &= -a_j(n-1)x_j(n)s(n) + \sum_{i=1}^{K} a_j(n-1) \\ &\quad \times \Big(\gamma_i(n-1)a_i(n-1)+\mu_i(n-1)\xi_i(n-1)\Big) \\ &\quad \times x_i(n)x_j(n) \\ &= -a_j(n-1)x_j(n) \\ &\quad \times \Bigg[s(n) - \sum_{i=1}^{K}\Big(\gamma_i(n-1)a_i(n-1) \\ &\qquad + \mu_i(n-1)\xi_i(n-1)\Big)x_i(n)\Bigg] \\ &= -a_j(n-1)x_j(n)e(n). \end{aligned} \tag{6}$$

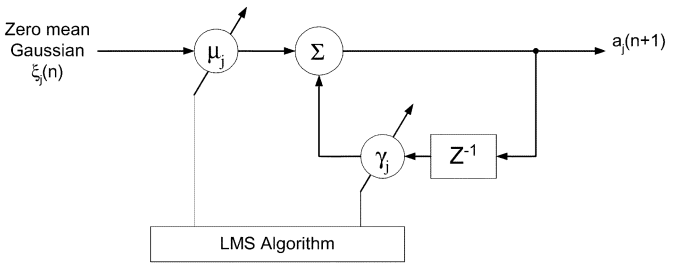

Fig. 3. Block diagram of the LMS adaptive MPA.

Therefore

$$\gamma_j(n+1) = \gamma_j(n) + \eta_\gamma \lfloor a_j(n-1)x_j(n)e(n) \rfloor. \tag{7}$$

For convergence purposes, the expectation of the model amplitude is expressed as

$$E\left(a_j(n+1)\right) = \gamma_j(n)E\left(a_j(n)\right) + \mu_j(n)E\left(\xi_j(n)\right). \tag{8}$$

If convergence is assumed such that $Lim_{n\to\infty} a_j(n) = a_j^*$, and since $E(\xi_j(n)) = 0$, then the expected steady-state value for the coefficient of the first-order Markov process would converge to $\gamma_j^* = 1$. Furthermore, to guarantee system stability, it can be shown that η_γ should satisfy the condition [17]

$$0 < \eta_\gamma < \frac{1}{\left(a_{\max}^*\right)^2 \lambda_{\max}} \tag{9}$$

where $a_{\max}$ is the maximum model amplitude of the first-order Markov process and $\lambda_{\max}$ is the maximum eigenvalue of the correlation matrix of oscillation signals, x_j.

Similarly, to adaptively adjust μ, it can be shown that

$$\hat{\nabla}_{\mu_j} J(n) = \begin{bmatrix} \frac{\partial e^2(n)}{\partial \mu_1(n1-)} \\ \vdots \\ \frac{\partial e^2(n)}{\partial \mu_K(n-1)} \end{bmatrix} = -\xi_j(n-1)x_j(n)e(n). \tag{10}$$

Therefore

$$\mu_j(n+1) = \mu_j(n) + \eta_\mu \lfloor \xi_j(n-1)x_j(n)e(n) \rfloor \tag{11}$$

where η_μ is a small positive constant called the adaptive learning rate which controls the speed of the adjustment. To guarantee model convergence, it can be shown that η_μ should satisfy the condition [17]

$$0 < \eta_\mu < \frac{1}{\lambda_{\max}}. \tag{12}$$

III. Results

EEG signals were recorded from nine rats using the experimental protocol described in Section II-A. The rats were divided into equal sized groups and subjected to 3-, 5-, and 7-min asphyxic CA injury. The performance of the AMPA method was determined by its capability to model EEG segments from the BL, ER, and LR phases satisfactorily since they have different statistical and spectral characteristics. The EEG and the random Gaussian, ξ, signals were filtered with a Butterworth second order low-pass filter with a cutoff frequency of 60 Hz. In each EEG segment, the proposed AMPA method was applied

TABLE I
NORMALIZED MAXIMUM CROSS CORRELATION BETWEEN MODEL AND ORIGINAL EEG SIGNALS FOR K FREQUENCIES

K	R(0)%
1	58
2	100
3	91
4	88

to selected stationary windows. For each window, the Welch's method was used to obtain the EEG PSD with frequency resolution equal to 0.25 Hz. To determine the optimum number of dominant frequencies K, the cross correlation function between the model output and the original signals was computed for different K values. In each experiment, the K dominant frequencies in the clinical bands were used. Table I shows the normalized maximum cross correlation value $R(0)$ obtained for each K indicating that $K = 2$ should be selected to obtain the best results. Two dominant frequency peaks in the spectrum confirms the result of Goel *et al.* [9] in similar brain injury studies. In a brain injury model of neonatal pigs, they observed three dominant peaks during EEG recovery.

The shaded areas of Fig. 4(a), (c), and (e) show the PSD of the normalized EEG signals recorded from one rodent representing the 5-minasphyxia during the BL, ER and LR segments, respectively. It was observed that the two dominant frequencies in the BL and ER segments were (3 and 12.5 Hz) and (5 and 9 Hz), respectively. For the LR period, the two dominant frequencies were (4 and 15 Hz). Fig. 4(b), (d), and (f) shows the normalized original and modeled EEG signals for the above three segments. The striking similarities between the original and the modeled signals reflect the capability of the model to simulate EEG signals under the three different conditions. The PSD was used as a measure of similarity between the original and modeled EEG signals. The PSD of the modeled EEG signal is represented by the dark line envelope shown in Fig. 4(a), (c), and (e).

To quantify the similarity between the actual and model output EEG signals, the MSE between their PSDs was calculated. The Percent normalized MSE was then calculated using

$$\text{NMSE} = \frac{\text{MSE}}{\text{Mean Signal Power}} \times 100\%. \tag{13}$$

The NMSE was found to be 12%, 13%, and 10% for BL, ER and LR segments, respectively. These NMSE values indicate that the modeling performance is acceptable. The corresponding NMSE values for the same EEG signals using the MPA [14] were found to be 28%, 32%, and 24%, respectively. The comparison of NMSE values reflects the advantage of using adaptive modeling over fixed parameter models.

The learning rates η_μ and η_γ were set to fixed values throughout training. The choice of the learning rates influenced the stability and speed of convergence of the adaptive model. Provided that (9) and (12) were satisfied to guarantee model stability, increasing the two rates was noticed to speedup the convergence and tracking signal variations.

After convergence, it was empirically found that the NMSE was far less sensitive to η_γ variations in comparison with η_μ.

To demonstrate the ability of the AMPA method to simulate fine nonstationary signal changes like bursts, Fig. 5 shows a 24-s strip of the original and modeled EEG data obtained from the ER segment.

The model's ability to track long EEG records that contain BL, SP, ER, and LR segments was also tested. Since the frequency contents of the EEG signal changes with time, a 1-min moving window was used to estimate the two dominant frequencies using the Welch's method. It was found that the frequencies of the rhythm generators were constant to within $\pm 5\%$ of the average values during the 1-min window.

Fig. 6 shows the original (top) and model output (bottom) EEG signals covering all segments: BL, SP, ER, and LR. The similarity between the two signals indicates the capability of the model in tracking the nonsationarites of the EEG signal at various stages before and after asphyxia.

Although that the EEG signal shown in Fig. 6 had three distinct domains of relatively long durations, each domain had a high degree of nonstationarity. AMPA was clearly not only able to track these long distinct domains but also was able to track transient EEG activities in the order of seconds as shown in Fig. 5.

The NMSE was also calculated for an EEG signal covering BL, SP, ER, and LR periods and was found to be 23% and 10% using MPA and AMPA methods, respectively. That indicates the improvement in modeling performance of the dynamic AMPA over the MPA method.

Further analysis of the model showed that the second derivative of γ, $\ddot{\gamma}$ amplified the spiking and bursting activity of the EEG signals relative to the background random EEG signal. To confirm this relationship between the spiking or bursting EEG and $\ddot{\gamma}$, consider the first derivative of (5) for a single frequency j

$$\begin{aligned}\dot{\gamma}_j(n+1) &= \gamma_j(n+1) - \gamma_j(n) = -\eta_\gamma \hat{\nabla}_{\gamma_j} J(n) \\ &= \eta_\gamma E\left[a_j(n-1)x_j(n)e(n)\right].\end{aligned} \tag{14}$$

Consequently

$$\begin{aligned}\ddot{\gamma}_j(n+1) &= \eta_\gamma E\Big[a_j(n-1)x_j(n)e(n) \\ &\qquad - a_j(n-2)x_j(n-1)e(n-1)\Big] \\ &= \eta_\gamma a_j^*\Big[E\left(x_j(n)s(n)\right) - E\left(x_j(n)y(n)\right) \\ &\qquad - E\left(x_j(n-1)s(n-1)\right) \\ &\qquad + E\left(x_j(n-1)y(n-1)\right)\Big] \\ &= \eta_\gamma a_j^*\Big[E\left(x_j(n)s(n)\right) \\ &\qquad - E\left(x_j(n-1)s(n-1)\right)\Big].\end{aligned} \tag{15}$$

Assuming that the spiking or bursting EEG occurred at time sample n such that the EEG signal is given by

$$s(n) = w(n) + g(n) \tag{16}$$

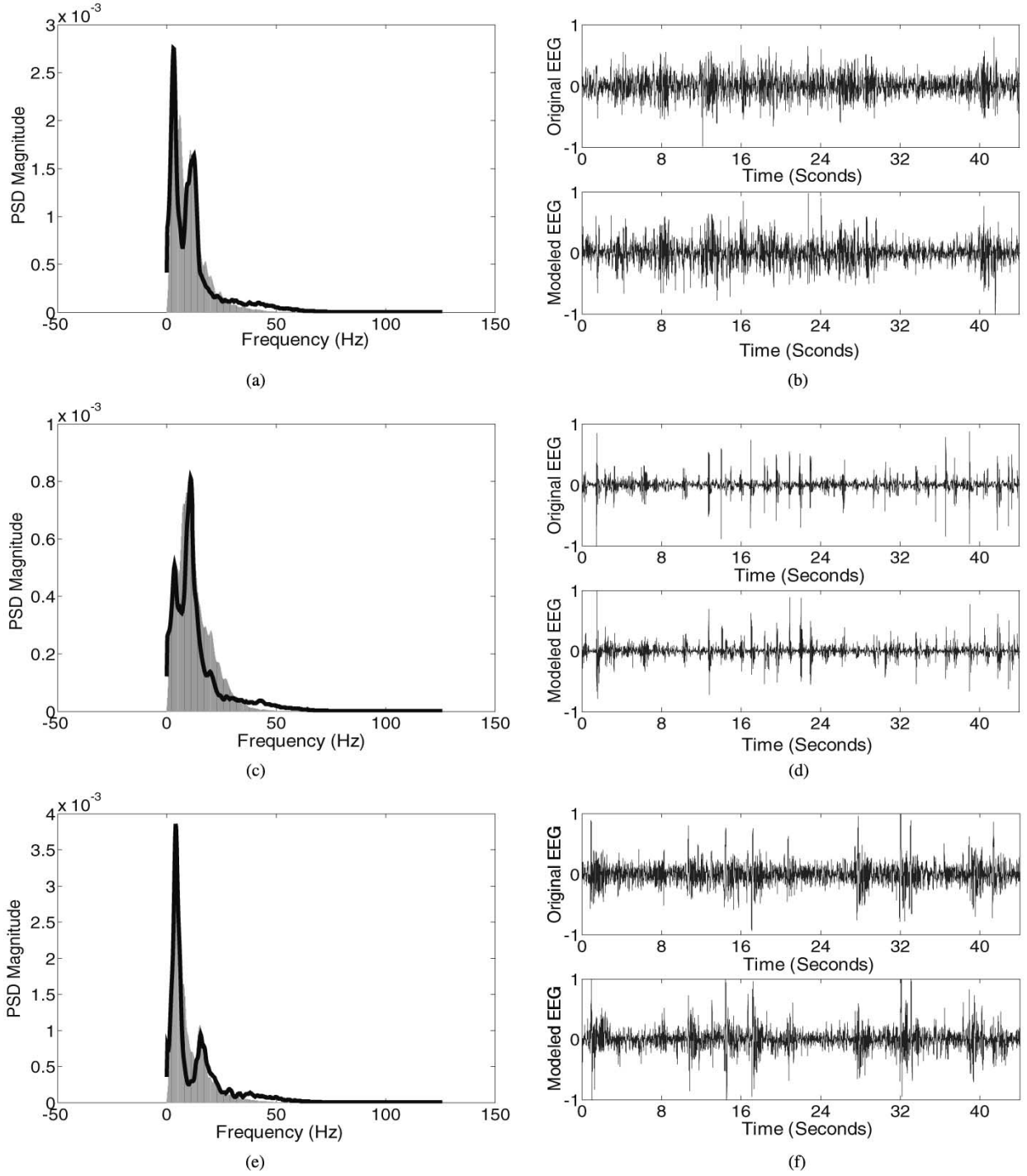

Fig. 4. (a), (c), (e) The PSD of the normalized original and simulated EEG signals for one rodent representing the 5 min of asphyxic arrest during the BL, ER, and LR segments, respectively. (b), (d), (f) The normalized original and modeled EEG signals for the three corresponding segments.

where w represents the background random activity and g represents the spiking or bursting activity while $s(n-1) = w(n-1)$, then

$$\ddot{\gamma}_j(n+1) = \eta_\gamma a_j^* E\left(x_j(n) g(n)\right). \tag{17}$$

Hence, $\ddot{\gamma}$ is a crosscorrelation function that depends on the presence of spikes or bursts. Therefore, the frequency contents of $\ddot{\gamma}$ would represent the presence and intensity of bursts and spikes only. Fig. 7(a) and (b) shows two EEG segments (top) and the corresponding $\ddot{\gamma}$ (bottom) containing spikes and bursts, respectively.

IV. Discussion

The spikes and bursts are known to influence or prognosticate the neurological outcome [2], [11]. Hence studying the dynamic and adaptive rate changes of $\ddot{\gamma}$ as obtained by the adaptive model hints to the different stages of recovery.

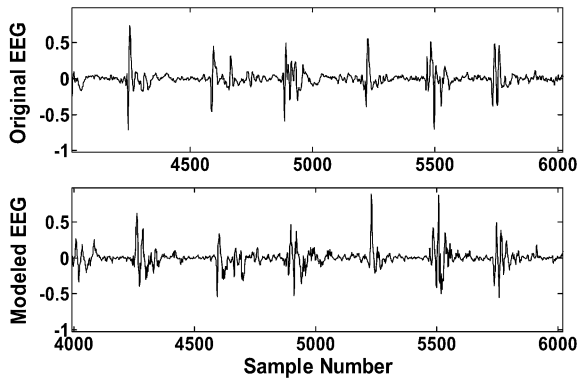

Fig. 5. An 8-s strip of the original and modeled EEG data obtained from the ER segment.

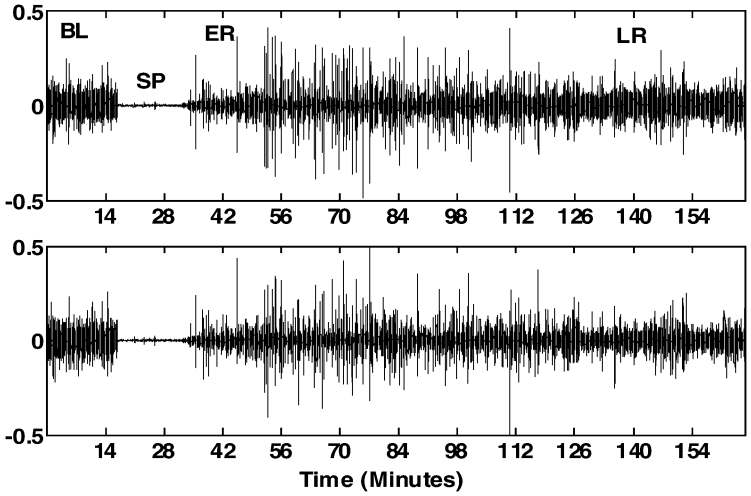

Fig. 6. Normalized original and modeled EEG signals covering BL, SP, ER, and LR periods.

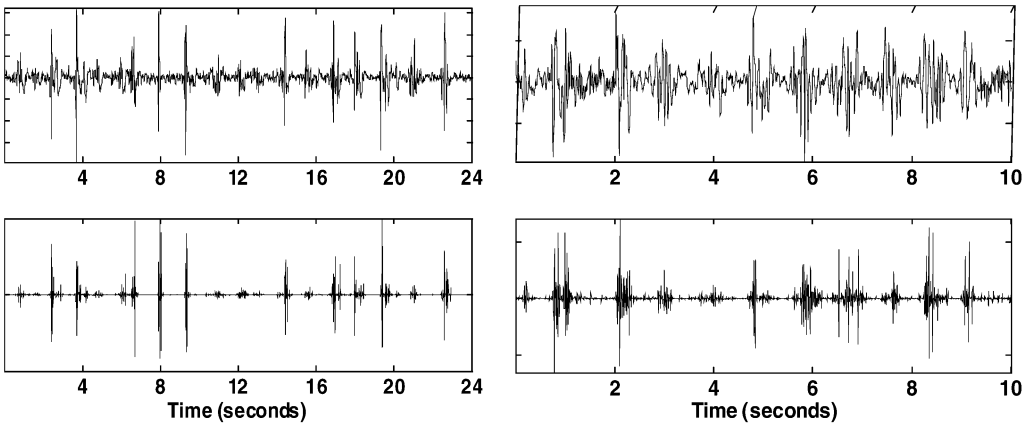

Fig. 7. EEG segments (top) and the corresponding $\ddot{\gamma}$ (bottom) containing (a) spikes and (b) bursts.

Although simple, the zero crossing rate (ZCR) of each time window of $\ddot{\gamma}$ was found to give such indications. In comparison with the actual EEG signal, higher ZCR coincided with the bursting activities while small ZCR represented the spiking EEG. Fig. 8(a)–(c) shows typical histogram of the ZCR of $\ddot{\gamma}$ for the whole recovery period following the SP for three rats that have been subjected to 3-, 7-, and 5-min of asphyxia, respectively. The x-axis represents the ZCR, while the y-axis represents the number of windows containing that ZCR.

Results obtained with 3-min asphyxia show the presence of relatively high ZCR for a considerable number of windows. It was noticed that all EEG signals recorded from the 3-min rats showed a short period of spiking activity followed by a gradual diffusion of these spikes turning into bursts. In comparison with the actual EEG signal, higher ZCR coincided with the bursting activities while small ZCR represented the spiking EEG. On the other hand, for the 7-min rats, a low ZCR was present throughout the recovery period indicating the presence

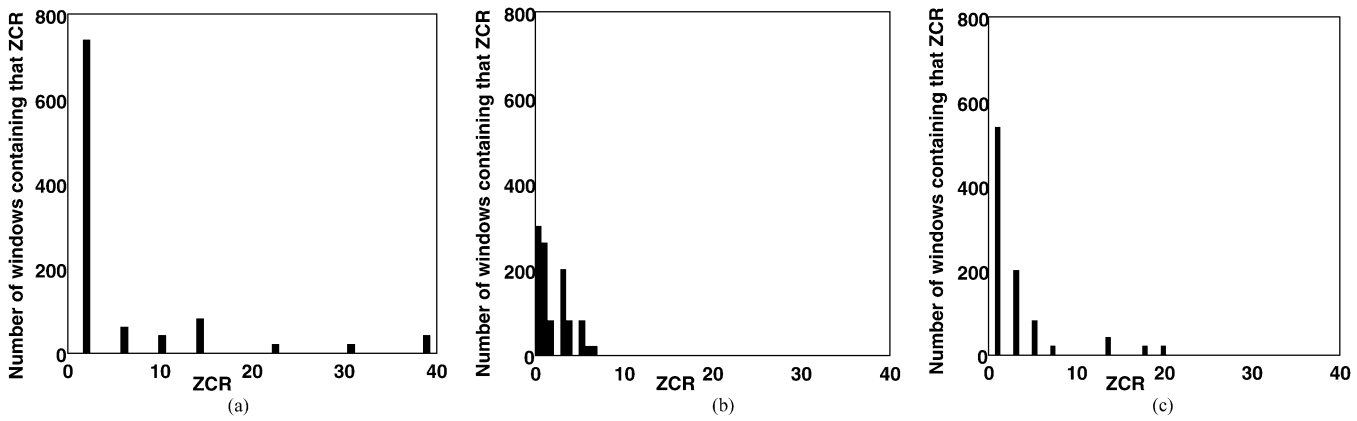

Fig. 8. ZCR histogram of $\ddot{\gamma}$ for the whole recovery period following the SP for (a) 3-min, (b) 7-min, and (c) 5-min asphyxia, respectively.

TABLE II
START TIME OF THE LR PHASE FOR THE NINE RATS SUBJECTED TO 3-, 5-, AND 7-MIN ASPHYXIA

Injury duration	Rat 1	Rat 2	Rat 3
3 minutes	88 minutes	101 minutes	93 minutes
5 minutes	Not detected	122 minutes	Not detected
7 minutes	Not detected	Not detected	Not detected

of spiking activity. The frequency of occurrence of these spikes was lower than the case of 3-min rats. For the 5-min cases, a mixture of ZCR patterns reflecting both the 3- and 7-min asphyxia were present.

It was estimated that for bursting, the average value for the ZCR was 20 with a standard deviation of 8. However, the spiking activity had an average ZCR of 5 with standard deviation of 2.5. Hence, a possible application where the above results might be utilized is the detection of the beginning of LR phase. Since the bursting activity is a clear indication of late recovery, a ZCR of 20 was used as a threshold value to determine the existence and the start of the LR phase. The ER phase was assumed to commence immediately following the SP with the detection of spiking activity. However, since the ER phase was present in the EEG of all experiments, the emphasis was on detecting the LR phase which is associated with a good neurological outcome. Table II shows the start time of the LR phase with reference to the start of the experiment for three groups of three rats each, subjected to 3-, 5-, and 7-min of asphyxic arrest. Although these observations are preliminary, evidently, the LR time period is delayed with increasing injury.

V. CONCLUSION

In this paper, the adaptive LMS algorithm with a first-order Markov process were used to model and simulate EEG signals recorded from rodent brains during injury and recovery following global cerebral ischemia. The generated AMPA model can be utilized to investigate the effectiveness of a certain quantitative EEG signal-analysis methods in segmenting different types of EEG signal patterns seen after recovery from brain injury. Results obtained from several rats show that the model was capable of simulating EEG signals recoded at different stages of injury and recovery. Analysis of the Markov model coefficients indicated that the frequency contents of their second derivative amplified the presence of spike and bursts in the EEG. Despite the encouraging preliminary results, the optimal choice of the adaptive learning rates and the cross coupling between dominant frequencies seen in the model are areas that need further investigation. The utilization of the AMPA method to generate EEG signals that simulate certain neurological activities is another challenging area of research. Segmentation of EEG by the AMPA method needs to show utility in diagnosis and therapy of patients with brain injury. This will be the subject of future clinical research and validation.

ACKNOWLEDGMENT

The authors thank A. Malhotra for providing the experimental support.

REFERENCES

[1] M. Thel and C. O'Connor, "Cardiopulmonary resuscitation: Historical perspective to recent investigations," *Amer. Heart J.*, vol. 137, pp. 39–48, 1999.

[2] D. Sherman, A. Bambrink, R. Ichord, V. Dasika, R. Koehler, R. Traystman, D. Hanley, and N. Thakor, "Quantitative EEG during early recovery from Hypoxic-Ischemic injury in immature piglets: Burst occurrence and duration," *Clin. Electroenceph.*, vol. 30, no. 4, pp. 175–183, 1999.

[3] A. Gevins and M. Aminoff, "Electroencephalography: Brain electrical activity," in *Encyclopedia of Medical Devices and Instrumentation*, J. Webster, Ed. New York: Wiley, 1988, pp. 1084–1107.

[4] E. Niedermeyer and F. Silva, *Electroencephalography : Basic Principles, Clinical Applications, and Related Fields*. Baltimore, MD: Williams & Wilkins, 1993.

[5] C. James and D. Lowe, "Using dynamical embedding to isolate seizure components in the ictal EEG," in *1st Int. Conf. Advances in Medical Signal and Information Processing 2000*, 2000, pub. no. 476, pp. 158–165.

[6] Z. Xu-Sheng, R. Roy, and E. Jensen, "EEG complexity as a measure of depth of anesthesia for patients," *IEEE Trans. Biomed. Eng.*, vol. 48, pp. 1424–1433, Dec. 2001.

[7] C. Borel and D. F. Hanley, "Neurological intensive care unit monitoring," in *Critical Care Clinics. Symposium on Neurological Intensive Care*, M. C. Rogers and R. J. Traysman, Eds. Philadelphia, PA, 1985, pp. 223–239.

[8] R. Agarwal, J. Gotman, D. Flanagan, and B. Rosenblatt, "Automatic EEG analysis during long-term monitoring in the ICU," *Electroenceph. Clin. Neurophysiol.*, vol. 107, pp. 44–58, 1998.

[9] V. Goel, A. Bambrink, A. Baykal, R. Koehler, D. Hanley, and N. Thakor, "Dominant frequency analysis of EEG reveals brain's response during injury and recovery," *IEEE Trans. Biomed. Eng.*, vol. 43, pp. 1083–1092, Nov. 1996.
[10] E. Niedermeyer, D. Sherman, R. Geocadin, H. Hansen, and D. Hanley, "The burst-suppression electroencephalogram," *Clin. Electroenceph.*, vol. 30, no. 3, pp. 99–105, 1999.
[11] R. Geocadin, R. Ghodadra, T. Kimura, H. Lei, D. Sherman, D. Hanley, and N. Thakor, "A novel quantitative EEG injury measure of global cerebral ischemia," *Clin. Neurophysiol.*, vol. 111, pp. 1779–1787, 2000.
[12] A. Bezerianos, S. Tong, A. Malhorta, and N. Thakor, "Information measures of brain dynamics," in *Nonlinear Signal and Image Processing Conf.*, Baltimore, MD, 2001.
[13] O. Rosso, S. Blanco, J. Yordanova, V. Kolev, A. Figliola, M. Schurmann, and E. Basar, "Wavelet entropy: A new tool for analysis of short duration brain electrical signals," *J. Neurosci. Methods*, vol. 105, pp. 65–75, 2001.
[14] O. Bai, M. Nakamura, A. Ikeda, and H. Shibasaki, "Nonlinear Markov process amplitude EEG model for nonlinear coupling interaction of spontaneous EEG," *IEEE Trans. Biomed. Eng.*, vol. 47, pp. 1141–1146, Sept. 2000.
[15] H. Al-Nashash, J. Paul, W. Ziai, D. Hanley, and N. Thakor, "Wavelet entropy for subband segmentation of EEG during injury and recovery," *Ann. Biomed. Eng.*, vol. 31, pp. 1–6, 2003.
[16] C. Vaz, X. Kong, and N. Thakor, "An adaptive estimation of periodic signals using a fourier linear combiner," *IEEE Trans. Signal Processing*, vol. 42, pp. 1–10, Jan. 1994.
[17] B. Widrow and S. Stearns, *Adaptive Signal Processing*. Englewood Cliffs, NJ: Prentice-Hall, 1985.
[18] L. Katz, U. Ebmeyer, P. Safar, and A. Radovsky, "Outcome model of asohyxial cardiac arrest in rats," *J. Cerebral Blood Flow Metab.*, vol. 15, pp. 1032–1039, 1995.

Hasan Al-Nashash (M'99–SM'03) received the B.Sc. degree in electronic engineering with medical electronics and the Ph.D. degree in electronic engineering from the University of Kent, Kent, U.K., in 1984 and 1988, respectively.

He served on the faculty of engineering at Mutah and Yarmouk Universities, Jordan, between 1988 and 1998, and since then he has been with the American University of Sharjah, UAE, where he is currently serving as an Associate Professor of Electrical and Electronic Engineering. His teaching and research interests are in the areas of electronics, medical instrumentation and signal and image processing. He developed several algorithms for ECG data classification and compression and currently is working on EEG signal analysis recorded during injury and recovery following global cerebral ischemia. He also developed an explosive anaerobic leg power meter and a pedobargraph for the detection of choreography feet position. He worked closely with several biomedical engineering departments and hospitals at Johns Hopkins University (Baltimore, MD), The American Hospital in Dubai (UAE), and Jordan University Hospital (Jordan).

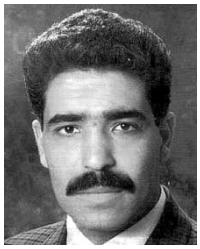

Yousef Al-Assaf received the B.Sc. degree from Sussex University, Brighton, U.K. and Ph.D. degree from Oxford University, Oxford, U.K. both in control engineering.

His research and industrial experiences are in the areas industrial instrumentation and control. During his work at Oxford University, he developed a computerized predictive controller for the cement mills for the Blue-Circle Cement factories. He was the Regional Manager and the University of Jordan Representative for one of the European Commission projects with the Mediterranean region (Euro-Mediterranean partnership). The aim of the project was to develop "a generic interactive package for systems engineering courses and applications." He participated in the establishment of the industrial engineering department at the University of Jordan and The Electrical and Computer Engineering programs at AUS. His areas of research interests include intelligent systems, adaptive and predictive control, and systems modeling and control.

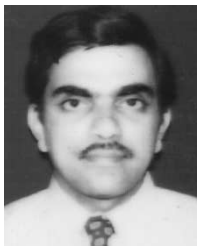

Joseph Paul graduated in electrical engineering (with distinction) from the University of Calicut, Kerala., India, in 1986 and received the M.Tech. and Ph.D. degrees in electrical engineering from the Indian Institute of Technology, Madras, India.

From 1987–1995, he was with the research division of Indian Telephone Industries, Bangalore, India. This paper was written while he was at the Johns Hopkins University School of Medicine, Baltimore, MD. Currently, he is serving as Assistant Professor in the Division of Bioengineering at the National University of Singapore. His research interests are biomedical instrumentation, neural signal processing, and neurophysiology of stroke models.

Nitish Thakor (S'78–M'81–SM'89–F'97) received the B.Tech. degree in electrical engineering from the Indian Institute of Technology, Bombay, India, in 1974 and the Ph.D. degree in electrical and computer engineering from the University of Wisconsin, Madison, in 1981.

He served on the faculty of Electrical Engineering and Computer Science of the Northwestern University, Evanston, IL, between 1981 and 1983, and since then he has been with the Johns Hopkins University, School of Medicine, Baltimore, MD, where he is currently serving as a Professor of Biomedical Engineering. He teaches and conducts research on cardiovascular and neurological instrumentation, medical microsystems, signal processing, and computer applications. He has authored more than 130 peer-reviewed publications on these subjects. He has recently established a Center for Neuroengineering at the Johns Hopkins University with the aim of carrying out interdisciplinary and collaborative engineering research for basic and clinical neurosciences. He is actively interested in developing international scientific programs, collaborative exchanges, tutorials, and conferences on neuroengineering and medical microsystems.

Dr. Thakor serves on the editorial boards of several journals, including the IEEE TRANSACTIONS ON BIOMEDICAL ENGINEERING, IEEE TRANSACTIONS ON INFORMATION TECHNOLOGY IN BIOMEDICINE, and *Annals of Biomedical Engineering*. He is a recipient of a Research Career Development Award from the National Institutes of Health and a Presidential Young Investigator Award from the National Science Foundation, and is a Fellow of the American Institute of Medical and Biological Engineering. He is also a recipient of the Centennial Medal from the University of Wisconsin School of Engineering and recognition from the students of the Alpha Eta Mu Beta Biomedical Engineering student Honor Society.